Vietnam Journal of Science and Technology ***58*** *(1) (2020) 119-129*

doi:10.15625/2525-2518/57/6/14278

FINITE ELEMENT MODELLING FOR VIBRATION RESPONSE OF CRACKED STIFFENED FGM PLATES

Do Van Thom[1, *], Doan Hong Duc[2], Phung Van Minh[1], Nguyen Son Tung[1]

[1]*Department of Mechanics, Le Quy Don Technical University, 236 Hoang Quoc Viet, Ha Noi, Vietnam*

[2]*Structures Laboratory, University of Engineering and Technology, 144 Xuan Thuy, Ha Noi, Vietnam*

[*]Email: *thom.dovan.mta@gmail.com*

Received: 20 August 2019; Accepted for publication: 2 December 2019

Abstract. This paper presents the new numerical results of vibration response analysis of cracked FGM plate based on phase-field theory and finite element method. The stiffener is added into one surface of the structure, and it is parallel to the edges of the plate. The displacement compatibility between the stiffener and the plate is clearly indicated, so the working process of the structure is described obviously. The proposed theory and program are verified by comparing with other published papers. Effects of geometrical and material properties on the vibration behaviours of the plate are investigated in this work. The computed results show that the crack and stiffener have a strong influence on both the vibration responses and vibration mode shapes of the structure. The computed results can be used as a good reference to study some related mechanical problems.

Keywords: finite element, phase-field theory, FGM, crack, stiffened plates, vibration.

Classification numbers: 5.4.3, 5.4.5, 5.4.6.

1. INTRODUCTION

The structures made from functionally graded materials (FGM) are used widely in engineering applications. These are smart materials which have many advantages than classical materials such as high strength, good performance in high temperature, wear-resistant, light weight and so on. However, they can appear cracks in the working process due to external forces. Hence, studying on the mechanical responses of FGM structures with cracks is a very important issue, in which the describing the crack in one structure in order to be convenient to analyze the mechanical system is the barrier. There have been many researches considering these problems. Rabczuk and Areias [1] used extended finite element method (X-FEM) to study the natural frequencies of FGM plate with cracks based on 4-noded field consistent enriched element. Natarajan *et al.* [2] used the extended finite element method to investigate the free vibration response of cracked functionally graded material plates. Chau-Dinh

et al. [3] applied phantom node method to carry out the mechanical behavior of shell with random cracks. Ghorashi *et al*. [4] employed an isogeometric analysis to examine the plate with cracks based on the T- spline basic functions. Kitipornchai *et al*. [5] researched the nonlinear vibration response of edge cracked FGM Timoshenko beams by using Ritz method. Huang *et al*. [6-8] used Ritz technique to explore the vibration of side-cracked FGM plate using the first-of-its-kind solutions. Huang *et al*. [9] investigated the vibration behavior of the cracked FGM plate based on the 3D theory of elasticity and Ritz methodology. Recently, phase-field method has been applied widely to study the structures with cracks; this new method presents an efficiency for both analyzing the structures with static cracks and dynamic cracks. The viewers can find the advantages of this method in [10-16].

This paper uses phase-field method to study the free vibration of FGM stiffened plate with and without cracks. The finite element formulations are derived based on first order shear deformation Mindlin plate theory. The numerical results show that the stiffeners have a strong effect on the free vibration of the structure. These computed data can be applied for engineers when analyzing and designing these types of structures in practice.

1. FORMULATION FOR FGM PLATE BASED ON REISSNER-MINDLIN THEORY

Consider an FG plate with a stiffener as shown in Figure 1. This paper employs Reissner-Mindlin plate theory, herein, the displacement field at any points of the structure can be expressed as follows:

$$\begin{aligned} u(x,y,z) &= u_0(x,y) + z\beta_x(x,y) \\ v(x,y,z) &= v_0(x,y) + z\beta_y(x,y)\,; \qquad (-h/2 \le z \le h/2) \\ w(x,y,z) &= w_0(x,y) \end{aligned} \tag{1}$$

where u,v,w are the vertical displacements along the x, y and z – axes at the coordinate z, respectively. β_x,β_y are the transverse normal rotations in the *xz*- and *yz*- planes. u_0,v_0,w_0 are the displacements at z = 0 (neutral surface).

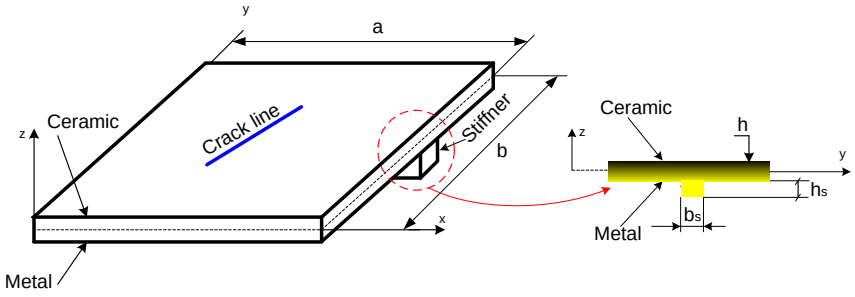

Figure 1. An FG plate with a stiffener.

At any points, three components (membrane strain $\boldsymbol{\varepsilon}_p$, bending strain $\boldsymbol{\varepsilon}_b$ and shear strain $\boldsymbol{\gamma}_s$) are expressed as follows

$$\boldsymbol{\varepsilon} = \begin{Bmatrix} \boldsymbol{\varepsilon}_p \\ \mathbf{0} \end{Bmatrix} + \begin{Bmatrix} z\boldsymbol{\varepsilon}_b \\ \boldsymbol{\gamma}_s \end{Bmatrix} \tag{2}$$

in which

$$\boldsymbol{\varepsilon}_p = \begin{Bmatrix} u_{0,x} \\ v_{0,y} \\ u_{0,y} + v_{0,x} \end{Bmatrix};\ \boldsymbol{\varepsilon}_b = \begin{Bmatrix} \beta_{x,x} \\ \beta_{y,y} \\ \beta_{x,y} + \beta_{y,x} \end{Bmatrix};\ \boldsymbol{\gamma}_s = \begin{Bmatrix} \beta_x + w_{0,x} \\ \beta_y + w_{0,y} \end{Bmatrix} \tag{3}$$

Assuming that the stiffener is parallel to the *Ox* axis, the displacement field of the stiffener at this time takes the form as follows

$$\begin{cases} u_s(x_1, y_1, z_1) = u_{s0}(x_1, y_1) + z\beta_{sx}(x_1, y_1) \\ w_s(x_1, y_1, z_1) = w_{s0}(x_1, y_1) \end{cases};\ \left(-h_s/2 \le z \le h_s/2\right) \tag{4}$$

The strain components of the stiffener are defined as follows

$$\varepsilon_{sm} = \frac{\partial u_{s0}}{\partial x};\ \varepsilon_{s\kappa} = \frac{\partial \beta_{sx}}{\partial x};\ \gamma_{s0} = \frac{\partial w_{s0}}{\partial x} + \beta_{sx} \tag{5}$$

The relationship between the strain field of the stiffener and the displacements field of the plate is shown in [17].

Herein, the elastic potential energy of the stiffened plate is expressed as follows

$$\begin{aligned} U(\mathrm{u}) = \frac{1}{2}\int_\Omega \left\{\boldsymbol{\varepsilon}_p^T \mathrm{A}_{pp}\boldsymbol{\varepsilon}_p + \boldsymbol{\varepsilon}_p^T \mathrm{A}_{pb}\varepsilon_b + \varepsilon_b^T \mathrm{A}_{pb}\boldsymbol{\varepsilon}_p + \varepsilon_b^T \mathrm{A}_{bb}\varepsilon_b + \boldsymbol{\gamma}_s^T \mathrm{A}_s \boldsymbol{\gamma}_s\right\} d\Omega + \\ \frac{1}{2}\int_L b_s h_s \left\{\varepsilon_{sm} E_s \varepsilon_{sm} + \varepsilon_{sm} E_s \varepsilon_{s\kappa} + \frac{h_s^2}{12}\varepsilon_{s\kappa} E_s \varepsilon_{s\kappa} + \gamma_{s0}\frac{E_s}{2(1+\nu_s)}\gamma_{s0}\right\} dl \\ = \int_\Omega \Psi(\mathrm{u})\, d\Omega \end{aligned} \tag{6}$$

where

$$\left\{\mathrm{A}_{pp},\ \mathrm{A}_{pb},\ \mathrm{A}_{bb}\right\} = \int_{-h/2}^{h/2} \frac{E(z)}{\left(1-\nu^2(z)\right)} \begin{bmatrix} 1 & \nu(z) & 0 \\ \nu(z) & 1 & 0 \\ 0 & 0 & \dfrac{(1-\nu(z))}{2} \end{bmatrix} \left\{1,\ z,\ z^2\right\} dz \tag{7a}$$

$$\mathrm{A}_s = \frac{5}{6}\int_{-0.5h}^{0.5h} \frac{E(z)}{2(1+\nu(z))} \begin{bmatrix} 1 & 0 \\ 0 & 1 \end{bmatrix} dz \tag{7b}$$

in which [10, 14, 18-19]

$$E(z) = E_m + (E_c - E_m)V_c;\ \nu(z) = \nu_m + (\nu_c - \nu_m)V_c\ ;\ V_c(z) = \left(\frac{1}{2} + \frac{z}{h}\right)^n;\ V_m = 1 - V_c \tag{8}$$

Herein, E_c, ν_c and E_m, ν_m are the Young's Modulus, Poisson ration of ceramic and metal, respectively. V_m and V_c are the volume fraction of metal ceramic. In this work, we assume that the stiffener is under the bottom surface of the plate and the stiffener is full of metal, so that $E_s = E_m$.

The kinetic energy of the stiffened FGM plate is expressed as

$$\mathrm{T} = \frac{1}{2}\int_\Omega \dot{\mathrm{u}}^T \rho_p \dot{\mathrm{u}} d\Omega + \frac{1}{2}\int_{\Omega_s} \dot{\mathrm{u}}_s^T \rho_s \dot{\mathrm{u}}_s d\Omega \tag{9}$$

where

$$\rho_p = \int_{-h/2}^{h/2} \left(\rho_m + \left(\rho_c - \rho_m\right)\right) dz;\ \rho_s = \int_{-h_s/2}^{h_s/2} \rho_m dz \tag{10}$$

The Lagrange functions can be now written in the form as

$$L(\mathrm{u}) = T(\mathrm{u}) - U(\mathrm{u}) \tag{11}$$

According to phase-field theory, the crack is the discontinuous region, which is described as a narrow zone by adding phase-field variation *s*. When *s* equals 0 means that the material is damaged and *s* equals 1 means that the material is not damaged. When phase-field variation *s* varies smoothly from 1 to 0, the crack is corresponding to the softening state of the material. Therefore, we can easily analyze the whole considered region, and it is convenient to integrate the crack area. This is the highlight point of phase-field approach comparing with other methods when solving numerous problems deal with cracks. Readers can see more detail in [10-13, 15-16, 20-22]. At this time, the energy function *L* of the stiffened plate with crack is written in the following form

$$\begin{aligned}
&L(\mathrm{u},s) = T(\mathrm{u},s) - U(\mathrm{u},s) = \frac{1}{2}\int_{\Omega_e} s^2 \dot{\mathrm{u}}^T \rho \dot{\mathrm{u}} d\Omega + \frac{1}{2}\int_{\Omega_s} \dot{\mathrm{u}}_s^T \rho_s \dot{\mathrm{u}}_s d\Omega \\
&-\frac{1}{2}\int_{\Omega} \left\{ \boldsymbol{\varepsilon}_p^T \mathrm{A}_{pp} \boldsymbol{\varepsilon}_p + \boldsymbol{\varepsilon}_p^T \mathrm{A}_{pb} \varepsilon_b + \varepsilon_b^T \mathrm{A}_{pb} \boldsymbol{\varepsilon}_p + \varepsilon_b^T \mathrm{A}_{bb} \varepsilon_b + \boldsymbol{\gamma}_s^T \mathrm{A}_s \boldsymbol{\gamma}_s \right\} d\Omega \\
&-\frac{1}{2}\int_L b_s h_s \left\{ \varepsilon_{sm} E_s \varepsilon_{sm} + \varepsilon_{sm} E_s \varepsilon_{s\kappa} + \frac{h_s^2}{12} \varepsilon_{s\kappa} E_s \varepsilon_{s\kappa} + \gamma_{s0} \frac{E_s}{2(1+\nu_s)} \gamma_{s0} \right\} dl \\
&-\int_{\Omega} G_C h \left[\frac{(1-\nu)^2}{4l} + l|\nabla s|^2 \right] d\Omega \\
&= \tilde{L}(\mathrm{u},s) - \int_{\Omega} G_C h \left[\frac{(1-\nu)^2}{4l} + l|\nabla s|^2 \right] d\Omega
\end{aligned} \tag{12}$$

where ∇s is the gradient of phase-field parameter. In this study, the crack is assumed throughout the thickness of the plate, thus, phase-field variation *s* does not change in the thickness direction, it only varies by the width of the crack (*s* varies smoothly from 0 to 1).

By minimizing the Lagrange function (12) we have

$$\begin{cases} \delta L(\mathrm{u}, s, \delta \mathrm{u}) = 0 \\ \delta L(\mathrm{u}, s, \delta s) = 0 \end{cases} \tag{13}$$

Then, we obtain the eigenvalue equation to determine the natural frequencies and the free vibration mode shapes of the stiffened FGM plate with cracks as follows

$$\begin{cases} \left(\sum \mathbf{K}^e + \omega^2 \sum \mathrm{M}^e\right)\mathrm{u} = 0 \\ \int_{\Omega} 2s.\tilde{L}(\mathrm{u})\delta s d\Omega + \int_{\Omega} 2G_C h \left[-\frac{(1-\nu)}{4l} + l\nabla s \nabla(\delta s) \right] d\Omega = 0 \end{cases} \tag{14}$$

The shape of the crack is defined by function $\tilde{L}(\mathrm{u})$ [23]

$$\tilde{L}(\mathbf{u}) = B\frac{G_J}{4l}.H(x) \tag{15}$$

where

$$H(x)=\begin{cases} 1 & if\ x\le c\ \ and\ \ \dfrac{-l}{2}\le y\le \dfrac{l}{2} \\ 0 & else \end{cases} \tag{16}$$

in which B is the coefficient with the value 10^3, and c is the length of the crack.

2. RESULTS AND DISCUSSION

3.1. Verification problems

Example 1: Firstly, the natural frequencies of this work and those of published papers are compared to one another to verify the proposed theory and finite element method for the FGM plate with a crack in case of clamped one edge. Consider a square plate a = b = 0.24 m, the thickness 0.00275 m, Young's modulus E = 6.7e10 Pa, Poisson's ratio 0.33, mass density 2800 kg/m^3. The plate has one crack of length 0.1416*a* at the location x = 9 cm, y= 9 cm. The non-dimensional natural frequencies from this work, [24] (experiment) and finite element method [25] are presented in Table 1. The results show that they meet a good agreement.

Table 1. The ratio ω_{crack} / ω_{no_crack} of the cantilever plate (ω_{crack} is eigen frequency of the cracked plate and ω_{no_crack} is eigen frequency of the plate without crack).

Mode	*c/H*	Ref. [24] theoretical	Ref.[24] experiment	Ref.[25] FEM	This work
1	0.1416	0.9931	0.9917	0.9891	0.9858
2	0.1416	0.9989	0.9981	0.9985	0.9935
3	0.1416	0.9837	0.9807	0.9826	0.9987

Example 2: Consider a fully simply supported rectangular plate with the dimension a = 0.41 m, b = 0.61 m, the thickness 0.00635 m. The plate has one stiffener along the short edge, the width of stiffener 0.0127 m, the height of stiffener 0.02222 m, Young's modulus E = 211 GPa, Poisson's ratio 0.3, the mass density 7830 kg/m^3. The non-dimensional natural frequencies are compared in Table 2. The comparison results in Table 2 show that the difference among the present results and other references is very small.

Table 2. The frequencies of the stiffened plate.

f_i (Hz)	Ref. [26]	Ref. [27]	Ref. [28]	Ref. [29]	Ref. [30]	This work
1	254.94	257.05	253.59	250.27	254.45	255.59
2	269.46	272.10	282.02	274.49	265.86	261.53
3	511.64	524.70	513.50	517.77	520.14	519.69

Example 3: Finally, we consider a fully simply supported square FGM plate made from (Si_3N_4/SUS304), the dimensions a = b = 0.2 m, h = 0.025 m. The material properties are as follows: metal SUS304: E_m = 207.79GPa, ν_m =0.3176, ρ_m =8166 kg/m^3, ceramic Si_3N_4: E_c = 322.27GPa, ν_c =0.24, ρ_c =2370 kg/m^3. The first three vibration frequencies of this work compared with the results by analytic methods [31-32], FEM [18] are shown in Table 3. We see that the comparison results are similar.

Table 3. First three natural frequencies of FGM plate, $\Omega_i = \left(\omega_i a^2 / h\right)\sqrt{\rho_m\left(1-\nu_m^2\right)/E_m}$.

Ω_i	n=0				n=0.5			
	[18]	[31]	[32]	This work	[18]	[31]	[32]	This work
Ω_1	12.498	12.507	12.495	12.239	8.554	8.646	8.675	8.439
Ω_2	29.301	29.256	29.131	28.691	20.559	20.080	20.262	19.749
Ω_3	45.061	44.323	43.845	43.439	31.088	29.908	30.359	29.861

3.2. Effects of some parameters on free vibration of stiffened cracked FGM plate

The following results are calculated for FGM plate made from Si_3N_4/SUS304 with the same material properties as in Example 3 above. The stiffener (made from metal SUS304) is set in the surface which is full of metal. The first free vibration frequencies are standardized by the formula $\Omega = \left(\omega_1 a^2 / h\right)\sqrt{\rho_m\left(1-\nu_m^2\right)/E_m}$.

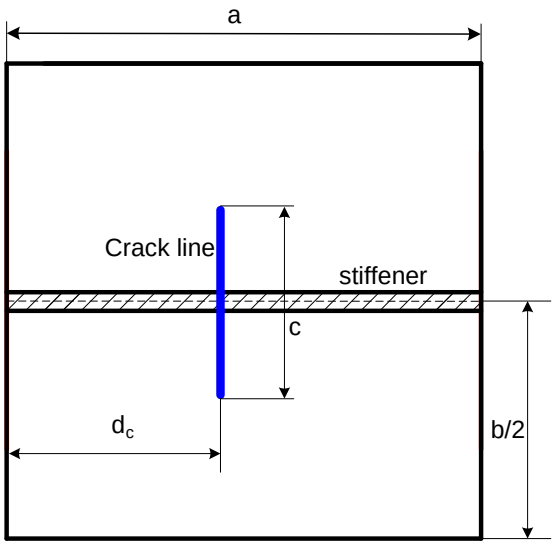

Figure 2. The geometry of the cracked FG plate with one stiffener.

- Consider a cracked plate with one stiffener (see Figure 2), a/b=1, h = a/100, the stiffener is in the center of the plate and parallel to one edge, the width of stiffener b_s = h, the height of stiffener h_s. The plate is fully simply supported. The distance from one edge to the crack is d_c, the length of the crack c = 0.3a and parallel to one edge of the plate.

In order to see more the effect of the location of the crack on the free vibration of the plate, we change the d_c so that d_c/a = 0.2-0.5, it means that the crack tends to move to the center of the plate. The normalized fundamental frequencies of the structure are shown in Table 4. From the results in this table, we find that when the crack is closer to the center of the plate, the plate becomes weaker, so the vibration frequencies of the plate decrease.

At the same time, when increasing the volume fraction index *n*, it will reduce the fundamental frequencies of the plate, this is because when increasing *n* will increase the metal proportion in the plate, the metal (SUS304) has a smaller elastic modulus than that of the ceramic (Si_3N_4), but the density of the metal is higher than the density of the ceramic, which leads to a reduction in the fundamental frequencies when *n* increases. Figure 3 shows the first four vibration mode shapes of cracked plate with different d_c/a ratios. From here we see that the crack has a great influence on both the fundamental frequencies as well as on vibration mode shapes of the plate.

Table 4. The normalized fundamental frequency (Ω) of cracked FGM plate with one stiffener as a function of the distance d_c, h_s/h ratios and gradient indexes *n* (c/a = 0.3).

d_c/a	h_s/h	*n*						
		0	0.2	0.5	1	2	5	10
-	0	12.840	10.368	8.869	7.810	7.0371	6.413	6.1174
0.3	1	12.157	9.905	8.510	7.514	6.783	6.189	5.905
	2	12.065	9.923	8.571	7.595	6.872	6.282	5.999
	3	12.027	9.968	8.646	7.682	6.964	6.374	6.089
	4	11.921	9.945	8.656	7.708	6.999	6.413	6.127
0.4	1	12.024	9.789	8.406	7.420	6.695	6.107	5.825
	2	11.830	9.718	8.386	7.426	6.715	6.135	5.856
	3	11.656	9.649	8.360	7.423	6.725	6.152	5.873
	4	11.445	9.538	8.295	7.383	6.700	6.137	5.862
0.5	1	11.976	9.749	8.370	7.386	6.664	6.078	5.796
	2	11.749	9.649	8.324	7.369	6.663	6.086	5.808
	3	11.537	9.546	8.269	7.340	6.649	6.081	5.805
	4	11.298	9.413	8.184	7.283	6.609	6.053	5.780

- In this section, we examine the effect of the length of the crack. Consider an FGM plate with two parallel stiffeners (they also parallel to one edge of the plate) as shown in Figure 4. There is one crack where it is parallel to stiffeners as shown in Figure 3. Let vary the length of the crack *c* so that c/a = 0-0.6. The fundamental frequencies are listed in Table 5. From the computed results we understand that when increasing the length of the crack, the plate becomes softer, thus, the fundamental frequencies of the structure reduce.

Mode	c/a=0 (No crack)	d_c/a = 0.3 c/a=0.3	d_c/a = 0.4 c/a=0.3	d_c/a = 0.5 c/a=0.3
1	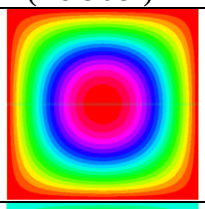	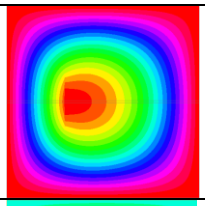	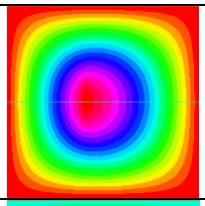	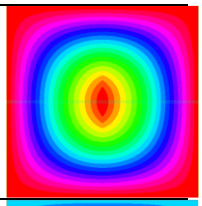
2	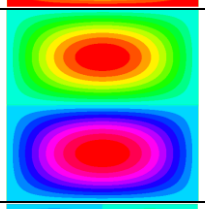	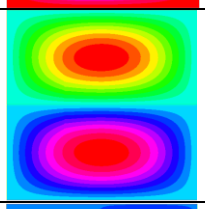	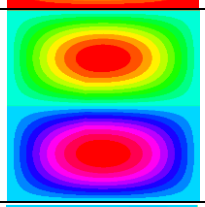	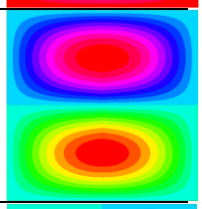
3	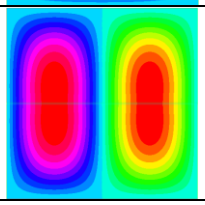	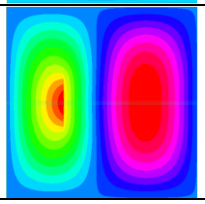	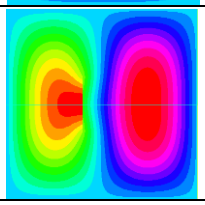	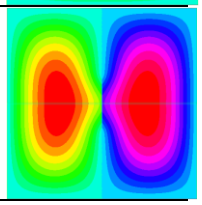
4	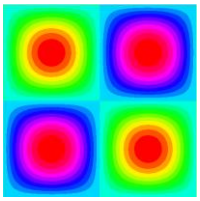	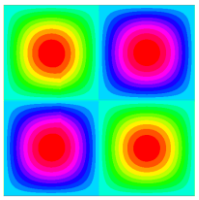	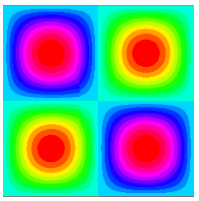	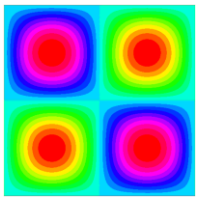

Figure 3. First four mode shapes of stiffened FG plate with one crack for different d_c/a ratios ($n = 0.5$, $h_s = 2h$).

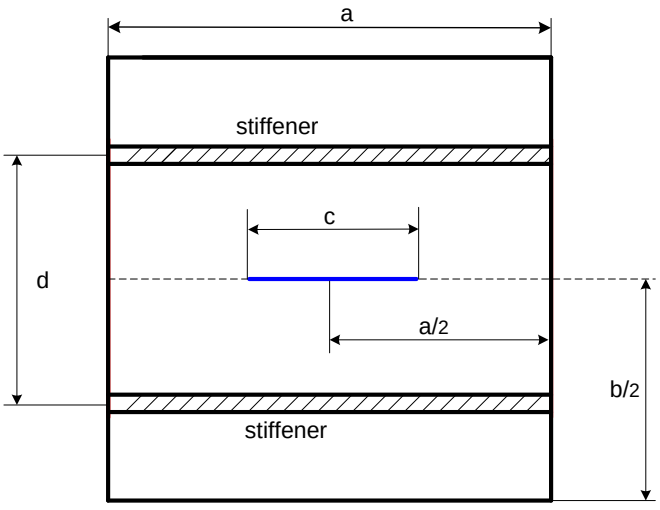

Figure 4. The geometry of the cracked FG plate with two stiffeners.

Table 5. The normalized fundamental frequency (Ω) of cracked FG plate with two stiffeners as a function of the crack length *c*, h_s/h ratios and gradient indexes *n* (*d*/*a* = 0.5, $\alpha = 0^o$).

c/*a*	h_s/h	*n*						
		0	0.2	0.5	1	2	5	10
0	0	12.840	10.368	8.869	7.810	7.0371	6.413	6.117
0.2	1	12.455	10.160	8.740	7.717	6.972	6.368	6.088
	2	13.001	10.748	9.327	8.293	7.530	6.910	6.628
	3	14.382	12.054	10.562	9.458	8.635	7.964	7.671
	4	16.486	13.974	12.337	11.106	10.181	9.424	9.107
0.4	1	11.891	9.677	8.308	7.334	6.618	6.038	5.762
	2	12.462	10.275	8.900	7.910	7.174	6.577	6.297
	3	13.842	11.568	10.114	9.054	8.256	7.607	7.311
	4	15.905	13.433	11.828	10.644	9.742	9.006	8.678
0.5	1	11.593	9.421	8.081	7.128	6.428	5.862	5.591
	2	12.176	10.025	8.676	7.704	6.984	6.399	6.125
	3	13.556	11.312	9.880	8.837	8.054	7.417	7.126
	4	15.600	13.151	11.565	10.397	9.509	8.785	8.462
0.6	1	11.330	9.188	7.874	6.940	6.256	5.703	5.442
	2	11.925	9.797	8.471	7.517	6.811	6.239	5.975
	3	13.308	11.078	9.667	8.641	7.872	7.246	6.970
	4	15.342	12.894	11.327	10.174	9.300	8.587	8.284

Table 6. The normalized fundamental frequency (Ω) of cracked FG plate with two stiffeners as a function of the distance between two cracks *d*, h_s/h ratios and gradient indexes *n* (*c*/*a* = 0.5).

d/*a*	h_s/h	*n*						
		0	0.2	0.5	1	2	5	10
-	0	12.840	10.368	8.869	7.810	7.0371	6.413	6.117
0.2	1	11.567	9.435	8.122	7.198	6.515	5.960	5.695
	2	12.555	10.563	9.271	8.321	7.603	7.015	6.745
	3	14.896	12.798	11.397	10.343	9.528	8.857	8.561
	4	18.082	15.771	14.185	12.968	12.009	11.213	10.869
0.4	1	11.557	9.426	8.103	7.158	6.464	5.900	5.631
	2	12.323	10.224	8.891	7.925	7.204	6.617	6.344
	3	14.077	11.878	10.452	9.401	8.604	7.953	7.659
	4	16.620	14.210	12.615	11.422	10.502	9.748	9.417
0.5	1	11.493	9.421	8.081	7.128	6.428	5.862	5.591
	2	12.176	10.025	8.676	7.704	6.984	6.399	6.125
	3	13.556	11.312	9.880	8.837	8.054	7.417	7.126
	4	15.600	13.151	11.565	10.397	9.509	8.785	8.462
0.6	1	11.422	9.414	8.058	7.097	6.394	5.826	5.553
	2	12.028	9.831	8.468	7.493	6.775	6.193	5.919
	3	13.019	10.746	9.319	8.291	7.527	6.907	6.620
	4	14.527	12.082	10.533	9.408	8.564	7.879	7.568

Finally, we investigate the effect of the distance between 2 stiffeners. First, changing the distance between them so that the dc/a ratio gets values from a range of 0.2 to 0.6 (c/a=0.5), the natural frequencies are listed in Table 6. We can easily see that, the higher the distance dc reaches, the softer the structure becomes. Therefore, the natural frequencies will reduce. The vibration mode shapes in 4 cases (plate with and without stiffeners, plate with and without cracks) are presented in Figure 5. Then, we can see that the crack, stiffener, and location of stiffener effect strongly on the free vibration of the structure.

Mode	$c/a = 0$, $h_s = 0$ (Plate with no crack and stiffener)	$d/a = 0.2$ $c/a = 0.5$, $h_s = 2h$	$d/a = 0.4$ $c/a = 0.5$, $h_s = 2h$	$d/a = 0.6$ $c/a = 0.5$, $h_s = 2h$
1		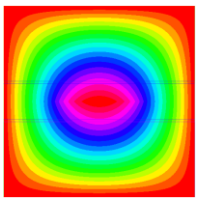	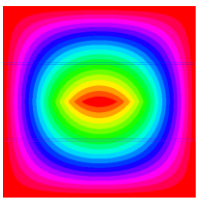	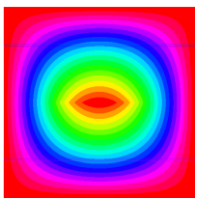
2	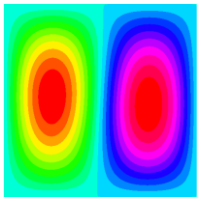	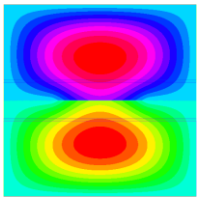	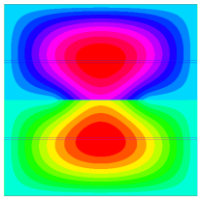	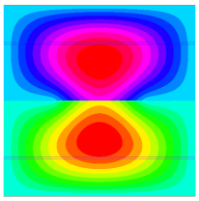
3	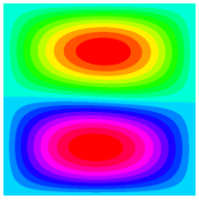	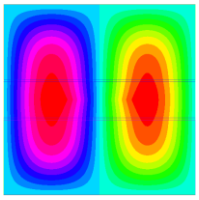	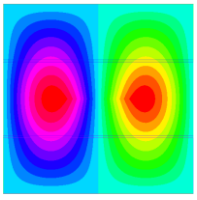	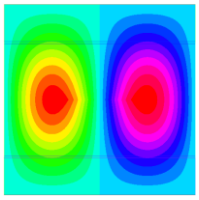
4	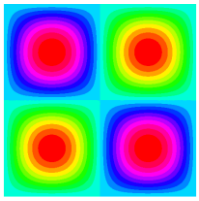	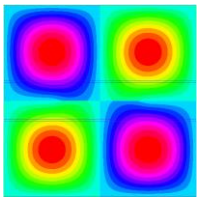	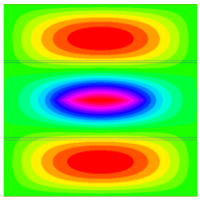	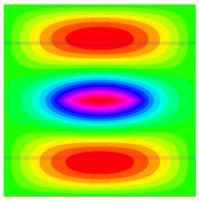

Figure 5. First four vibration mode shapes of FG plate with one crack and two stiffeners for different d/a ratios ($n = 0.5$).

4. CONCLUSIONS

This paper uses phase-field theory to establish the calculation equations of free vibration problems of stiffened FGM plate with cracks based on first order shear deformation Mindlin

plate theory and finite element method. The proposed method is verified through comparing with other published papers with three cases: FGM plate, FGM plate with stiffeners, FGM plate with cracks. In this work, we carry out the vibration responses of cracked FGM plate with one and more stiffeners. Effects of some parameters such as the distance between two stiffeners, the location of the stiffener, the length of stiffener, etc., on the free vibration of the structure are investigated. From the numerical results we have some remarkable conclusions as follows:

- When increasing the length of the crack, the plate becomes softer, thus, the natural frequencies of the structure decrease. The same phenomenon also appears when the crack tends to extend near the center of the structure.

- In case of the plate has 2 stiffeners, when increasing the distance between them, the plate also becomes softer and the natural frequencies will decrease, correspondingly.

- In addition, the appearing of the crack and the interaction between the crack and stiffener will effect strongly on the vibration mode shapes of the structure.

Acknowledgments. DVT gratefully acknowledges the support of Vietnam National Foundation for Science and Technology Development (NAFOSTED) under grant number 107.02-2018.30.

REFERENCES

1. Rabczuk T. and Areias P., M., A. -A meshfree thin shell for arbitrary evolving cracks based on an external enrichment, Comput. Model. Eng. Sci. **16** (2006) 115–130.
2. Natarajan S., Baiz P. M., Bordas S., Rabczuk T. and Kerfridena P. -Natural frequencies of cracked functionally graded material plates by the extended finite element method, Compos. Struct. **93** (2011) 3082–3092.
3. Chau-Dinh T., Goangseup Zi., Phill-Seung L., Rabczuk T. and Jeong-Hoon S. - Phantom-node method for shell models with arbitrary cracks, Comput. Struct. **92–93** (2012) 242–256.
4. Ghorashi S. Sh., Valizadeh N., Mohammadi S. and Rabczuk T. - T-spline based XIGA for fracture analysis of orthotropic media," Comput. Struct. **147** (2015) 138–146.
5. Kitipornchai S., Ke L. L., Yang J. and Xiang Y. - Nonlinear vibration of edge cracked functionally graded Timoshenko beams, J. Sound Vib. **324** (2009) 962–982.
6. Huang C. S., Leissa A. W. and Chan C. W. - Vibrations of rectangular plates with internal cracks or slits, Int. J. Mech. Sci. **53** (2011) 436–445.
7. Huang C. S., Leissa A. W. and Li R. S. - Accurate vibration analysis of thick, cracked rectangular plates, J. Sound Vib. **330** (2011) 2079–2093.
8. Huang C. S., McGee O. G. and Chang M. J. - Vibrations of cracked rectangular FGM thick plates, Compos. Struct. **93** (2011) 1747–1764.
9. Huang C. S., McGee O. G. and Wang K. P. - Three-dimensional vibrations of cracked rectangular parallelepipeds of functionally graded material, Int. J. Mech. Sci. **70** (2013) 1–25.
10. Thom V.D., Duc H.D., Duc N.D. and Tinh Q.B. - Phase-field thermal buckling analysis for cracked functionally graded composite plates considering neutral surface, Comp. Struct. **182** (2017) 524-548.

11. Duc HD, Tinh QB, Thom VD, Duc ND. - A rate-dependent hybrid phase field model for dynamic crack propagation, J. Appl. Phys. **122** (2017) 115102 1-4.
12. Duc N.D., Truong T.D., Thom V.D. and Duc H.D. - On the Buckling Behavior of Multi-cracked FGM Plates, Procd. Inter. Conf. Adv. Comp. Mech. 2017, Lecture Notes in Mechanical Engineering: 29-45.
13. Phuc M.P., Thom V.D., Duc H.D. and Duc N.D. - The stability of cracked rectangular plate with variable thickness using phase-field method, Thin-Wall. Struct. **129** (2018) 157-165.
14. Reddy J.N. - Analysis of Functionally Graded Plates, Inter. J. Num. Meth. Eng. **47** (2000) 663-684.
15. Miehe C., Hofacker M. and Welschinger F. - A phase field model for rate-independent crack propagation: robust algorithmic implementation based on operator splits, Comp.Meth. Appl. Mech. Eng. **199** (2010) 2766-2778.
16. Bourdin B., Francfort G.A. and Marigo J.J. - The variational approach to fracture, J. Elast. **91** (2008) 5–148.
17. Nam V.H., Duc H.D., Nguyen M.K., Thom V.D. and Hong T.T. - Phase-field buckling analysis of cracked stiffened functionally graded plates. Comp. Struct. **217** (2019) 50-59.
18. Tinh Q. B., Thom V. D., Lan H. Th. T., Duc H. D., Satoyuki T., Dat T. Ph., Thien-An Ng.V., Tiantang Y. and Sohichi H. - On the high temperature mechanical behaviors analysis of heated functionally graded plates using FEM and a new third-order shear deformation plate theory, Comp. part B **92** (2016) 218-241.
19. Thom V.D., Tinh Q.B., Yu T.T., Dat P.T. and Chung T.N. - Role of material combination and new results of mechanical behavior for FG sandwich plates in thermal environment, J. Comp. Sci. **21** (2017) 164-181.
20. Doan H.D., Bui Q.T., Nguyen D.D. and Fushinobu K. - Hybrid phase field simulation of dynamic crack propagation in functionally graded glass-filled epoxy, Comp. Part B. **99** (2016) 266-276.
21. Michael J.B., Clemens V.V., Michael A.S., Thomas J.R.H. and Chad M.L. - A phase-field description of dynamic brittle fracture, Comp. Meth. Appl. Mech. Eng. **217–220** (2012) 77–95.
22. Josef K., Marreddy A., Lorenzis L.D., Hector G. and Alessandro R. - Phase-field description of brittle fracture in plates and shells, Comp. Meth. Appl. Mech. Eng. **312** (2016) 374-394.
23. Borden M.J., Verhoosel C.V., Scott M.A., Hughes T.J.R., Landis C.M.- A phase-field description of dynamic brittle fracture. Comp. Meth. Appl. Mech. Eng. **217-220** (2012) 77–95.
24. Krawczuk M. and Gdansk. - Natural vibrations of rectangular plates with a through crack, Arch. Appl. Mech. **63** (1993) 491-504.
25. Qian G.L., Gu S.N. and Jiang J.S. - A finite element model of cracked plates application to vibration problems, Comp. Struct. **39** (1991) 483-487.
26. Aksu G. - Free vibration analysis of stiffened plates by including the effect of inplane inertia, J. Appl. Mech. **49** (1982) 206–212.
27. Mukherjee A. and Mukhopadhyay M. - Finite element free vibration of eccentrically

stiffened plates, Comp. Struct. **30** (6) (1988) 1303–1317.

28. Harik I.E., Guo M. - Finite element analysis of eccentrically stiffened plates in free vibration, Comp. Struct. **49** (6) (1993) 1007–1015.
29. Bhimaraddi A., Carr A.J., Moss P.J. - Finite element analysis of laminated shells of revolution with laminated stiffeners, Comp. Struct. **33** (1) (1989) 295–305.
30. Peng L.X., Liew K.M. and Kitipornchai S. - Buckling and free vibration analyses of stiffened plates using the FSDT mesh-free method, J. Sound Vibr. **289 (**2006) 421-449.
31. Wattanasakulpong N., Prusty G.B. and Kelly D.W. - Free and forced vibration analysis using improved third-order shear deformation theory for functionally graded plates under high temperature loading, J. Sandw. Struct. Mater. **15** (2013) 583-606.
32. Huang X.L. and Shen H.S. - Nonlinear vibration and dynamic response of functionally graded plates in thermal environments, Int. J. Solids Struct. **41** (2004) 2403-2427.